Journal of Forestry Research (2011) 22(2): 249–257
DOI 10.1007/s11676-011-0158-8

ORIGINAL PAPER

The impact of climate change on forest fire danger rating in China's boreal forest

YANG Guang • DI Xue-ying • GUO Qing-xi • SHU Zhan • ZENG Tao
YU Hong-zhou • WANG Chao

Received: 2010-06-06; Accepted: 2010-07-22

Abstract: The Great Xing'an Mountains boreal forests were focused on in the northeastern China. The simulated future climate scenarios of IPCC SRES A2a and B2a for both the baseline period of 1961–1990 and the future scenario periods were downscaled by the Delta Method and the Weather Generator to produce daily weather data. After the verification with local weather and fire data, the Canadian Forest Fire Weather Index System was used to assess the forest fire weather situation under climate change in the study region. An increasing trend of fire weather severity was found over the 21st century in the study region under the both future climate change scenarios, compared to the 1961–1990 baseline period. The annual mean/maximum fire weather index was predicted to rise continuously during 2010–2099, and by the end of the 21st century it is predicted to rise by 22%–52% across much of China's boreal forest. The significant increases were predicted in the spring from of April to June and in the summer from July to August. In the summer, the fire weather index was predicted to be higher than the current index by as much as 148% by the end of the 21st century. Under the scenarios of SRES A2a and B2a, both the chance of extremely high fire danger occurrence and the number of days of extremely high fire danger occurrence was predicted to increase in the study region. It is anticipated that the number of extremely high fire danger days would increase from 44 days in 1980s to 53–75 days by the end of the 21st century.

Foundation project: This research was supported by the "Eleventh Five-Year" National Science and Technology Support Project (2006BAD04B05), National Forestry Public Benefit Research Foundation (No.200804002) and the Youth Foundation of Northeast Forestry University (No.09051).

The online version is available at http:// www.springerlink.com

YANG Guang • DI Xue-ying (✉)• GUO Qing-xi • SHU Zhan
ZENG Tao • YU Hong-zhou • WANG Chao
College of Forestry, Northeast Forestry University, Harbin 150040, P.R. China. E-mail: dixueying@126.com

Responsible editor: Yu Lei

Keywords: climate change; wildfire; boreal forest; fire weather species; West Africa

Introduction

As one of the largest terrestrial biomes in the world, the boreal forest, which accounts for approximately 30% of the world's forested areas, plays an important role in the global cycling of energy, carbon and water (Conard and Ivanova 1997). The study region in the Great Xing'an Mountain Range (GXAMR) is the most important boreal forest in China, and it is also the most southern part of the global boreal forest biome.

Forest fires are strongly influenced by weather and climate (Flannigan and Harrington 1988; Johnson 1992; Swetnam 1993). Therefore, forest fire is one of the most important climate change impacts on the boreal forest now and in future because of its dominant role in interacting with other impacts (Wheaton 2001). With approximately 0.15 million hectares burned annually, the fire occurrence in GXAMR is relatively less extensive than the average level of the global boreal forest (Flannigan et al. 2005). Due to the proactive fire suppression policy carried out by the forest administration in the region for the past two decades, all forest fires were put out immediately after the ignition was detected. As a result, fuel was rapidly built up in the study region, and it became a serious concern as fuel means with higher fire risk and more severe damage. The accumulation of deadwood and debris across the continuous boreal forest landscape in GXAMR could result in severe forest fires in the region, which may be too difficult and too costly to suppress (Andrews et al. 2007).

It is generally accepted that the global temperature is increasing with the largest increase happening at high latitudes in the Northern Hemisphere where boreal forest resides (Soja et al. 2007). Climate change projection indicates that GXAMR is likely to become hotter and drier in the future; therefore, un-

der-standing interactions between the climatic influence and the characteristics of forest fire regimes is essential for fire management in the region. Studies demonstrates that forest fires are influenced by the changing climate (Westerling et al 2006; Ly and Tian 2007; Lavorel et al. 2007; Running 2006; Pausas 2004; Mollicone et al. 2006). A number of studies focused on the possible impacts of global warming on wildland fires using the General Circulation Models (GCMs), which can be used to project future climate change, the impact of this change on fire weather severity (Flannigan et al. 2005; Pino et al. 1998; Stock et al. 1998; Hennessy et al. 2006), and potential changes in areas burned due to climate change (Stocks et al. 1998; Tymstra et al. 2007; Flannigan et al. 2005). All these studies were conducted in temperate regions of the western US, Australia and the boreal forests in Canada or Russia. As an important component of the global boreal forest, the boreal forest in China's GXAMR region needs a similar study to assess possible associations between forest fire and climate change.

The Canadian Forest Fire Weather Index System (CFFWIS) is used to quantitatively measure fire risk for the study region. With daily temperature, relative humidity, precipitation, and wind speed as input, CFFWIS can be used to keep track of the forest's day-to-day susceptibility to fire (Van Wagner 1987). The system is comprised of several standard output components. The first three are fuel moisture codes that follow daily changes in the moisture contents of three layers of forest fuel with different drying rates. The last three components are the fire behavior indexes representing the rate of fire spread, fuel weight consumption and fire intensity. The system depends solely on weather readings taken each day on temperature, relative humidity, wind speed and precipitation (if any) during the previous 24 hours. Three fuel moisture codes are the Fine Fuel Moisture Code (FFMC), Duff Moisture Code (DMC), and Drought Code (DC). The Fire Weather Index (FWI) is derived from the fuel moisture codes and weather readings. FFMC, DMC, DC and FWI are arranged in code form with values rising as the moisture content decreases or the fire danger increases. There are two other outputs from the system: the Daily Severity rating (DSR) and the Seasonal Severity rating (SSR). In general, FWI reflects the fire danger and is usually used as fire hazard warning. DSR is a measure on the difficulty of fire control (Di 1993), and SSR is an index representing the seasonal mean of fire control difficulty (Flannigan et al. 2000). FWI is adopted as a comprehensive measure of forest fire danger in the study region.

The purpose of this study is to assess potential changes in forest fire weather risk influenced by climate. This change in risk is related to forest fire activities such as fire occurrence, area burned, and the impact of such changes on fire activities in the GXAMR region. Such information is very critical for medium to make long term forest management plan in the region. To achieve this goal, the weather data collected from the region's weather stations from 1950s to 2000s were used. Then, GCMs are used to simulate future weather conditions until the end of 21st century under two climatic change scenarios of the Hadley Center Coupled Model 3–A2a and B2a (Gordon et al. 2000; Pope et al. 2000). The simulated daily weather conditions such as daily temperature, relative humidity, wind speed and precipitation are then used as input to CFFWIS to generate FWI, which reflects daily fire risk. The simulated FWI provides a long term trend of forest fire potentials in the region, and is an important reference for assessing the region's forest fire risk under the global climatic change scenarios, most likely to occur in the future.

Materials and methods

Study area descriptions

The GXAMR region is located in the northeastern China bounded by 50°10'N–53°33'N and 121°12'E–127°00'E with a total area of 8.35 million ha (Fig. 1). The region locates in the cool temperate and a terrestrial monsoon climate zone with mean annual temperature of -2.8°C and mean annual precipitation of 746 mm. The forest landscape in this region is dominated by Xing'an larch (*Larix gmelini*), and other major tree species are Asian white birch (*Betula platyphylla*), Scot pine (*Pinus sylvestris var. mongolica*) and Mongolian oak (*Quercus mongolica*) (Heilongjiang Yearbook Editorial Board 2008; Jiang et al. 2002).

Data collection

Meteorological data

Meteorological data are collected from 18 weather stations in and around the study region, and the data comprises of daily, monthly and annual observations on temperature, wind speed, relative humidity and precipitation. Among 18 weather stations, seven are located inside the study region, and the other 11 stations are in the surrounding area (Fig. 2). Interpolation is used to generate grid data of weather factors for the later modeling exercise. The purpose of selecting the data from the surrounding areas is to make the interpolated results more accurate. The weather data was downloaded from China's meteorological data sharing service system. The availability of the weather data is listed in Table 1, in which there are the time and type of the data available. The data are not complete for all 18 weather stations, and some data are missing in several stations for certain time periods. For example, there are missing data in Tahe station for 1962–1971 and in Mohe station in 1958. Therefore, one-dimensional linear regression method has to be used to fill in the data gaps.

Climatic scenarios

The data for the climate change scenario in this study include the observed mean monthly values of mean/maximum temperature, total precipitation, wind speed and relative humidity for 1961–1990 (referred to as 1980s). The projected mean monthly values are used for 2010–2039 (referred to as 2020s), 2040–2069 (referred to as 2050s), and 2070–2099 (referred to as 2080s). The four periods have the same length of 30 years. The projection is done by using the third version of the Hadley Center Coupled Model (HadCM3). As the most commonly used projection

method, HadCM3 requires no flux adjustment or the stable climate in global mean, and it demonstrates to perform better than other models for Eastern Asia, where China is located. The scenarios tested belong to the A2 and B2 storylines and the families of A2a and B2a, respectively. In particular, the A2a storyline family describes a very heterogeneous world, presuming self-reliance and preservation of local identities. The B2a storyline emphasizes the local solutions to economic, social, and environmental sustainability (Leckebusch and Ulbrich 2004).

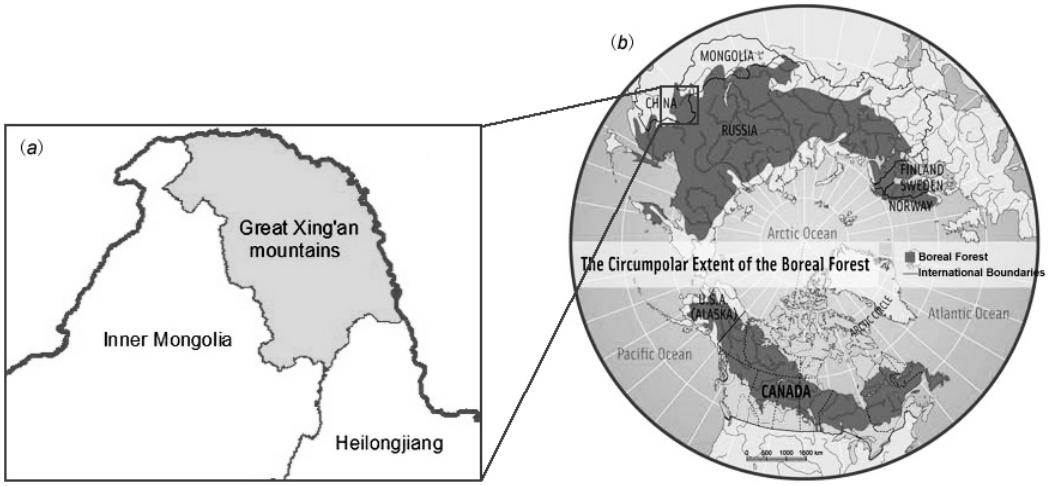

Fig. 1 (a): the geographic location of the study region; (b): the northern circumpolar of the global boreal forest.

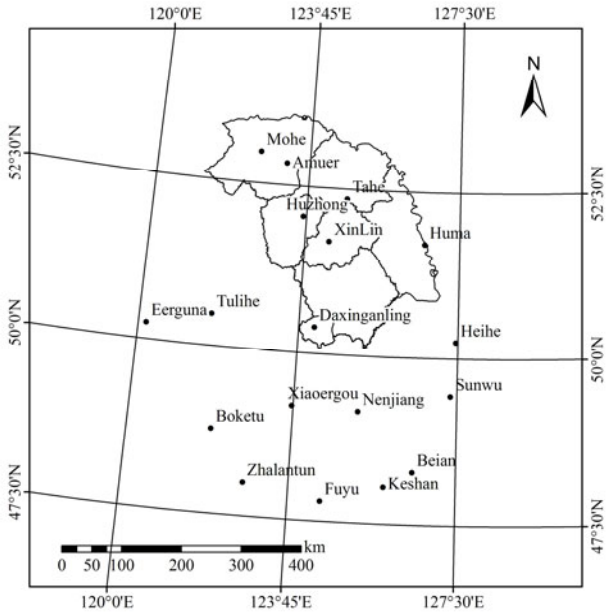

Fig. 2 The grid boundary for conducting the HadCM3 model analysis that covers the study region and 18 weather stations. The grid of interpolation has 1000 rows and 1000 columns with the spatial resolution of 40 m × 40 m.

Statistical analyses

Delta change methods

Generally, the spatial resolution of the output from GCMs like HadCM3 is coarse and not suitable for representing regional climate/weather situations. Therefore, downscaling is needed to make the resolution finer to meet the regional scale requirement. In the last decade, downscaling techniques for both dynamic and statistical approaches were developed. The coarse spatial resolution can thus be made finer in the studies of climate change scenarios.

Table 1. Data type and availability

Weather variable	The data type and the time period when the data available		
	Annual, 1951–2008	Monthly, 1961–1990	Daily, 1951–2008
T (°C)	Mean T Maximum T T anomaly	Mean T Maximum T ——	Maximum T —— ——
RH (%)	Mean RH	Mean RH	Mean RH
P (mm)	P P anomaly (%)	P Number of days with P ≥ 0.1 mm	20-20h P ——
W (m/s)	Mean W	Mean W	Mean W

T: Temperature; RH: Relative humidity; P: Precipitation; W: Wind speed.

The Delta change method (Akhtar et al. 2008; Zhao and Xu 2007) is recommended by the Global Change Research Program of the United States. This is a simple and useful method to generate future climate variables by combining previous observations and the simulated results through the HadCM3 model. The method is successfully used in many studies on the impact of climate change (Akhtar et al. 2008). The weather data used as the input to the Delta change method are the observations of temperature, relative humidity, wind speed and precipitation from 18 weather stations covering from 1961 to 1990. The future monthly values of the four weather variables were constructed using Eq.

1–4 as follows for each grid cell in the study region:

$$T_f = T_o + \left(\overline{T}_f - \overline{T}_o\right) \quad (1)$$

$$P_f = P_o\left(\overline{P}_f \overline{P}_o^{-1}\right) \quad (2)$$

$$R_f = R_o\left(\overline{R}_f \overline{R}_o^{-1}\right) \quad (3)$$

$$W_f = W_o\left(\overline{W}_f \overline{W}_o^{-1}\right) \quad (4)$$

Where, T_f is the monthly temperature for 12 × 30 months in each of the three future scenario periods (2020s, 2050s and 2080s). T_o is the observed monthly temperature for 12 × 30 months in the baseline period of 1961–1990. $\overline{T}_f$ is the mean of the future monthly temperature generated from the HadCM3 model for the future scenario periods, and $\overline{T}_o$ is the mean of the monthly temperature for the baseline period. The other three equations are used for deriving monthly precipitation, relative humidity and wind speed for the future scenario periods. The variables in the equations with the same subscripts as the ones in Eq. 1 denote the same time period.

Weather generator

CFFWIS requires the daily weather conditions of temperature, precipitation, relative humidity and wind speed as input, and the weather data coming from the Delta method is monthly. Hence, we need to generate daily weather data based on the monthly information for the future scenario periods. Weather generators are computational tools to produce daily and site-specific climate change scenarios (Semenov et al. 1998). One of the most commonly used weather generators is WGEN by Richardson and Wright (1984). It is chosen to produce daily weather data for each of the future scenario periods. WGEN produces synthetic daily time series of a group of climate variables such as maximum temperature, precipitation, relative humidity and wind speed with certain statistical properties. The monthly temperature, precipitation, relative humidity and wind speed are among the input to WGEN. The observed daily data and the daily data generated through WGEN for the baseline period were compared and tested at each weather station, and the test results showed there are low errors between the two data sources. Also, the serial correlation and cross serial correlations among the generated data are acceptable. For example, the relationships between the observed and the WGEN generated temperature and relative humidity for the baseline period for the Mohe weather station are shown in Fig. 3, showing a strong correlation between the observed and generated data. To convert point data of 18 weather stations to the grid data covering the study region, the ordinary Kriging analyses of the Geostatistical Analyst extension of the ESRI ArcGIS software (Yost et al. 1982; Chien et al. 1997) is applied in the study, and it is the most flexible Kriging model because it assumes a constant but unknown mean.

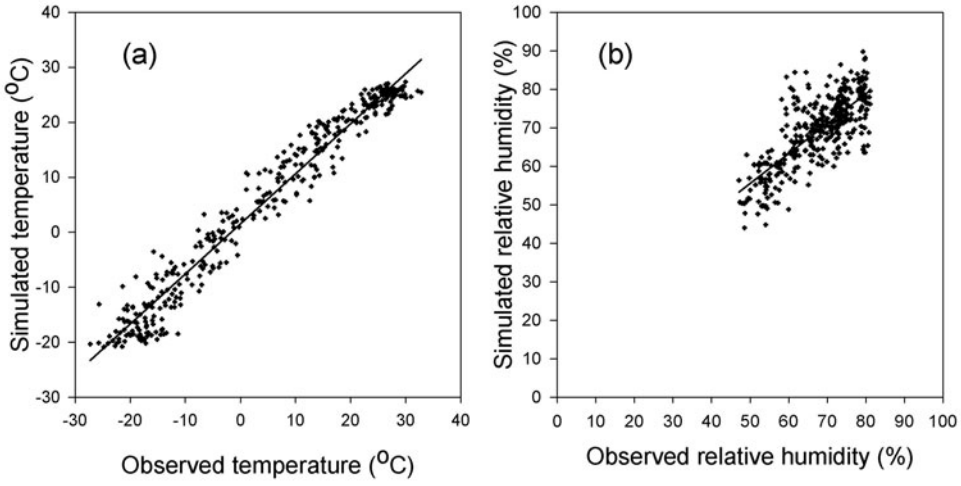

Fig. 3 (a): Scatter plot of observed and simulated daily maximum temperatures for the Mohe Weather Station. (b): Scatter plot of observed and simulated daily relative humidity for the Mohe Weather Station. The simulated data are based on the HadCM3 model and the WGEN model and for 1966–2008.

Testing FWI

FWI was used to link weather and climate conditions to fire hazards (Wheaton 2001). The system was once used in the study region during 1981–1991, but other studies suggested the system could be directly applied to boreal forests without the need for local calibration (Stocks et al. 1998; Willis et al. 2001; Tian et al. 2006). FWI is used to make daily fire hazard projections for each of the three future scenario periods based on the daily weather information generated from the WGEN method. Before FWI is used, the system is first tested by using both local weather data and fire data, which are provided by the local forest administration. The fire data for testing covers that in 1966–2008, including fire ignition time, ignition location, cause and area burned. The test results indicate that a significant correlation (r = 0.91) exists

between the annual mean FWI and annual fire occurrences (Fig. 4), although the correlation between the FWI and annual area burned is poor.

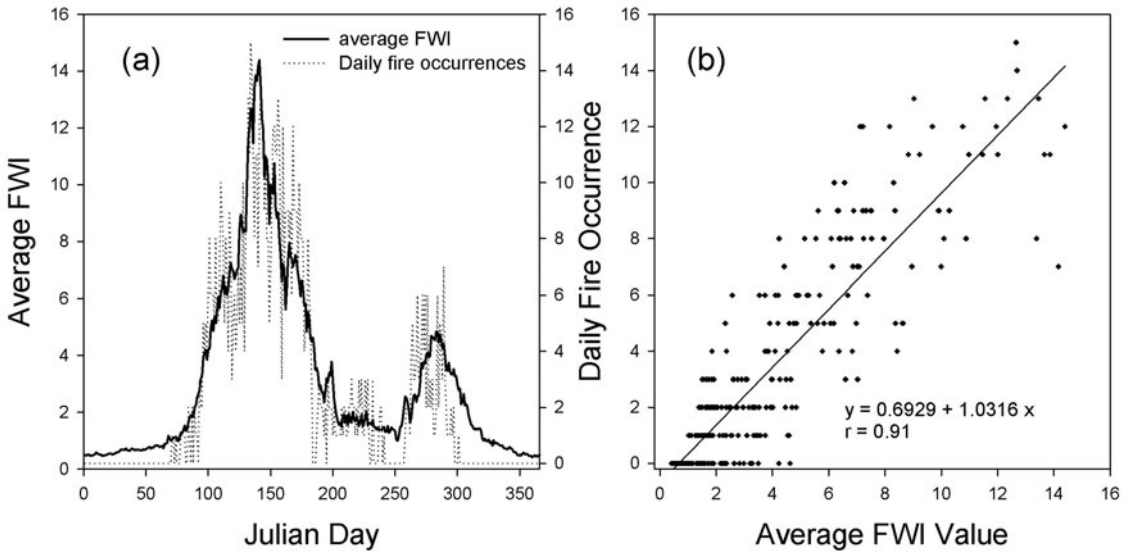

Fig. 4 (a): Scatter plot of the mean daily FWI and the mean daily fire occurrences versus Julian day for 1966–2008. (b): Scatter plot of the mean daily fire occurrence versus the mean daily FWI values for 1966–2008.

Results and discussion

In the study region, annual mean temperature increased by approximately 2.0°C since the 1950s (Fig. 5a), which is substantially greater than the global average increase. HadCM3 reflects that the annual mean temperature will potentially increase by 4.7°C under the A2a scenario, and it also reflects that the annual mean temperature will increase by 3.9°C under the B2a scenario during 2010–2099 in the study region. The projected precipitation also showed an increasing trend during the period (Fig. 5b): a 30% increase was under the A2a scenario, and a 16% increase was under the B2a scenario. It was observed that since 1959 the annual mean temperature anomaly exhibited an increasing trend during the fire season (April–October), with the highest positive anomaly occurring by the end of the 1980s (Table 2). Coupled with the rising temperature anomaly, the annual precipitation anomaly percentage also shows an increasing trend during the fire season for 1959–2008, although the increase is slight (Table 2).

Table 2. Summary of the proportions of fire activities corresponding to the fire danger classes during 1966–2008.

Weather variables	Time period				
	I	II	III	IV	V
Annual mean temperature anomaly (°C)	-4.53	-4.03	-2.55	4.72	5.85
Precipitation percentage anomaly (%)	0.15	-5.65	-0.93	6.95	0.44

I: 1959–1968; II: 1969–1978; III: 1979–1988; IV: 1989–1998; V: 1999–2008

In the study region, there were 36 fire occurrences burning 0.15 million ha on average annually during 1966–2008. A large forest fire occurred in the region on May 6, 1987, which lasted for 25 days and burned 1.01 million ha, causing huge economic and ecological damage (National Bureau of Statistics and Ministry of Civil Affairs 1995). When the fire data between the two periods of 1966–1987 and 1988–2008 were compared, both fire occurrence and burned area showed significant decrease after the 1987 large fire incident. The average of annual fire occurrence during 1988–2008 decreased by 31.4% compared to that in 1966–1987, the annual average burned area decreased by 77.7%, and the annual average burned forest decreased by 86.7%. However, in 1988–2008, the overall fire activities became more severe, with considerable variation in the magnitude of both fire occurrence and area burned (Fig. 6a). This may be attributed to the warming climate. During the fire season, fire activities concentrated in the spring months of March to May, and in the autumn months of September and October (Fig. 6b). However, the fire trend changed after entering the 21st century, with more fires occurring between July and August during 2001–2008. For example, 33.1% of all fires occurred during the summer months in this period, while only 3.8% of all fires occurred in summer in 1966–2000.

The emphasis of this study is on FWI and its changing trend under different climate change scenarios for the three future periods. Although the projected FWI is a daily time series for the three future time periods, it is also examined at annual and monthly scales. The annual mean FWI was calculated at all weather stations and interpolated to generate maps as shown in Fig. 7. Under the scenario A2a, the annual mean FWI will increase by approximately 5% in the 2020s, 18% in the 2050s, and

46% in the 2080s, compared to that in the baseline period. Under the scenario of B2a, the annual mean FWI will decrease by 3% in the 2020s, but increase by 24% in the 2050s, and by 26% in the 2080s, compared to that in the baseline period. The annual maximum FWI was calculated, and the results indicate that it will continue to increase for 2010–2099. In the 2080s, it will increase by as much as 52% under Scenario A2a and 22% under Scenario B2a. As for the monthly time scale, almost all monthly mean FWI demonstrates an increasing pattern under the two climate change scenarios for the three future periods compared to that in the baseline period (Fig. 8). The plots in the figure show the peaks at May and June, but the highest increase of the FWI happens in July and August. For example, under Scenario A2a, the monthly mean FWI will increase by 29% to 41%, compared to that in the 1980s. The same FWI will increase to 148% by the end of the 21st century. April will be subject to the second highest increase of the monthly average FWI, with the FWI going up by 50% in the 2080s.

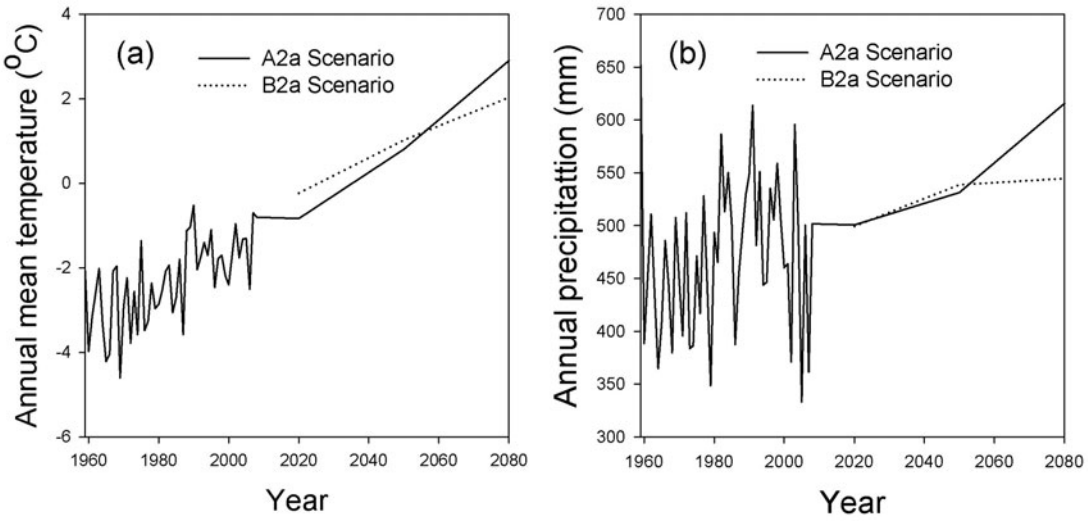

Fig. 5 (a): Observed (1959–2008) and projected (the three future periods under the two climate change scenarios) annual mean temperatures. (b): Observed (1959–2008) and projected (the three future periods under the two climate change scenarios) annual precipitations.

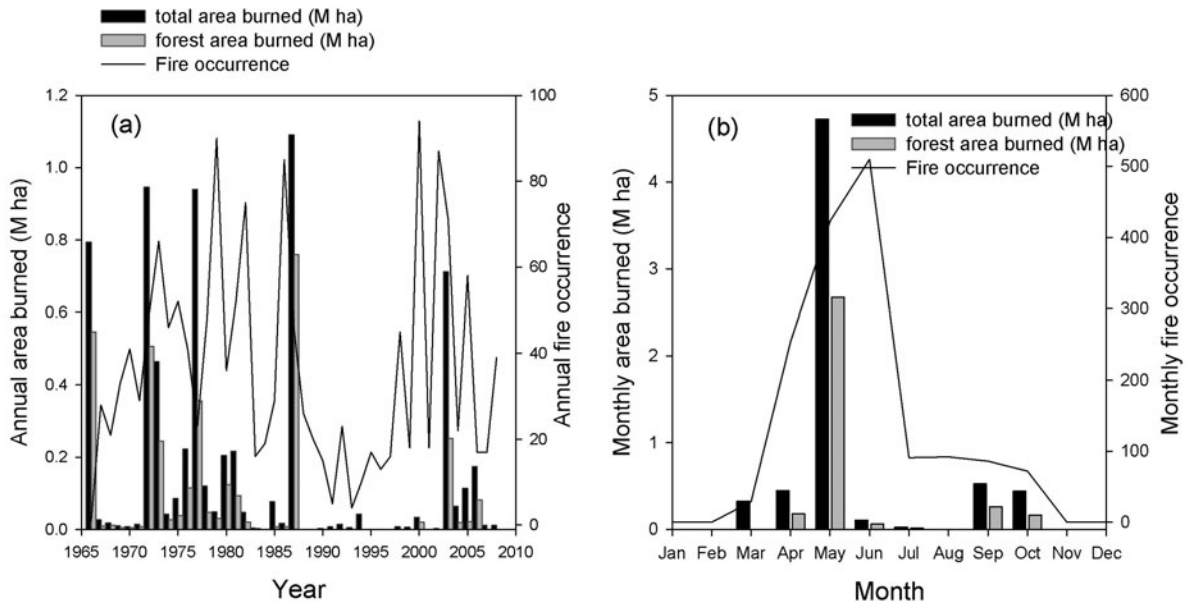

Fig. 6 (a): Time series of annual fire occurrence and area burned based on the observed data for 1966–2008. (b): Time series of monthly fire occurrence and area burned base on the observed for 1966–2008.

It is customary to use an ordinal variable to rank fire danger on different levels from low danger to extreme high danger for informing the general public. Fire danger was ranked into five categories according to the FWI values as presented in Table 3.

The ranking is based on FWI values, and the fire activities corresponding to the FWI ranks are also presented. Based on the ranking scheme, the daily FWI value is calculated for all three future periods under the two climate change scenarios, and it is classified into five fire danger classes (Fig. 9). In general, the number of low fire danger days will decrease and the number of extremely high danger days will increase for the three future periods of 2020s, 2050s and 2080s under both climate change scenarios. In the 1980s, on average there were 37 days of very high fire danger, and the number of days is predicted to double by the end of the 21st century. In the entire baseline period, there were a total of 44 days of extremely high fire danger; and in the 2080s this number will increase to 75 days under the A2a scenario and to 53 days under the B2a scenario.

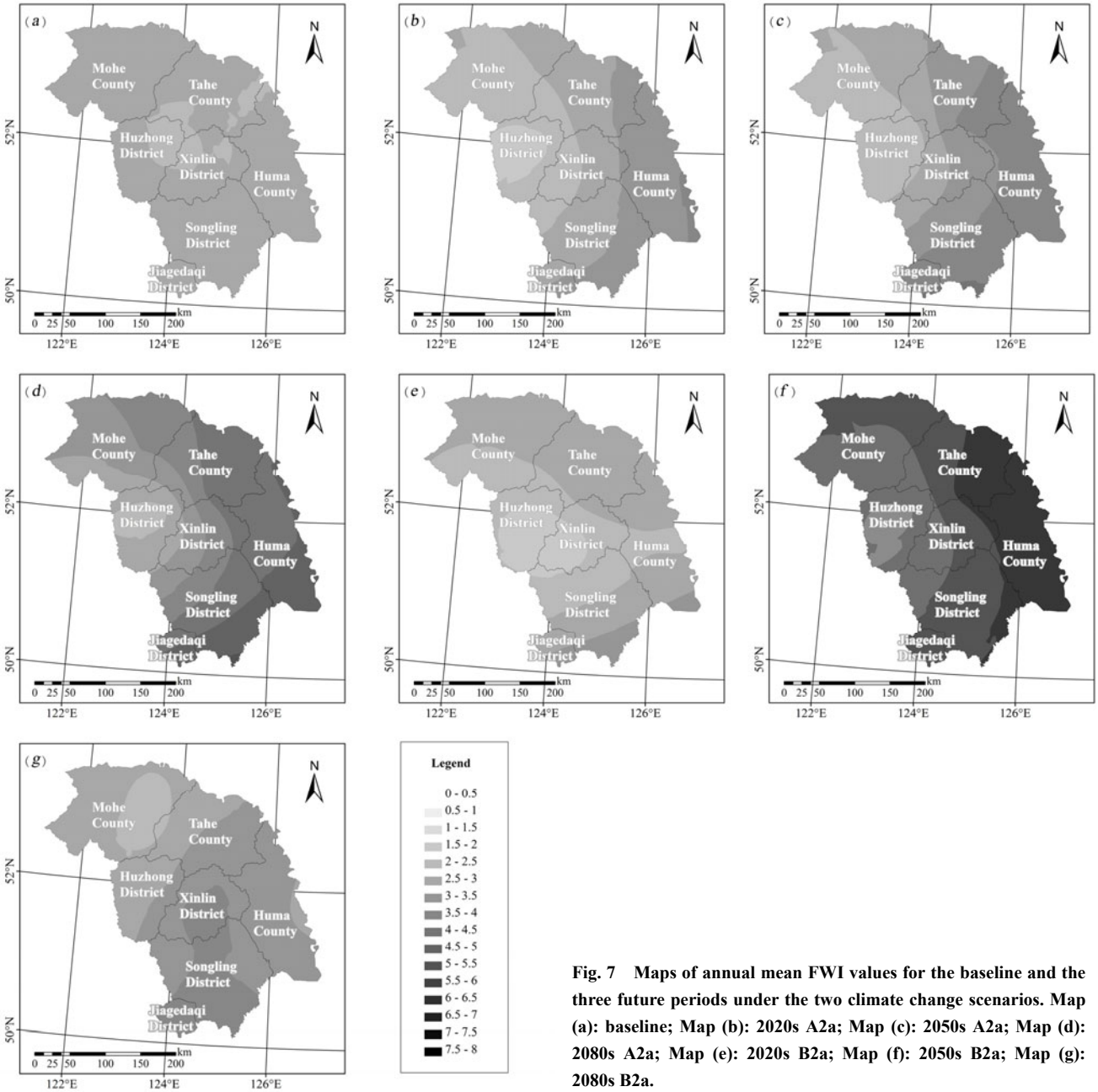

Fig. 7 Maps of annual mean FWI values for the baseline and the three future periods under the two climate change scenarios. Map (a): baseline; Map (b): 2020s A2a; Map (c): 2050s A2a; Map (d): 2080s A2a; Map (e): 2020s B2a; Map (f): 2050s B2a; Map (g): 2080s B2a.

Conclusion

In the study region, the annual mean temperature increased by approximately 2.0°C in the past 50 years, and the increase is likely to intensify in the 21st century. According to the HadCM3 model, the annual precipitation would increase by 16% to 30% in 2080s under both climate change scenarios. Since 1959, the anomaly of annual mean temperature in the fire season exhibied a large increase, and the number of extremely hot days also raised. In contrast, the precipitation showed a slight increase as indicated by the anomaly of annual precipitation percentage.

Forest fires and their characteristics are strongly influenced by weather and climate. In the study region, it was noted that increasing climate warming substantially increased fire activities such as fire occurrence, area burned and fire size since 2000. Although most of the forest fires occurred in spring and autumn in 1966–2000, the recent evidence indicated that the fire pattern changed and more forest fires occurred in the summer since 2000: 33.1% of fires occurred in summer since 2000 and 3.8% in summer during 1966 and 2000.

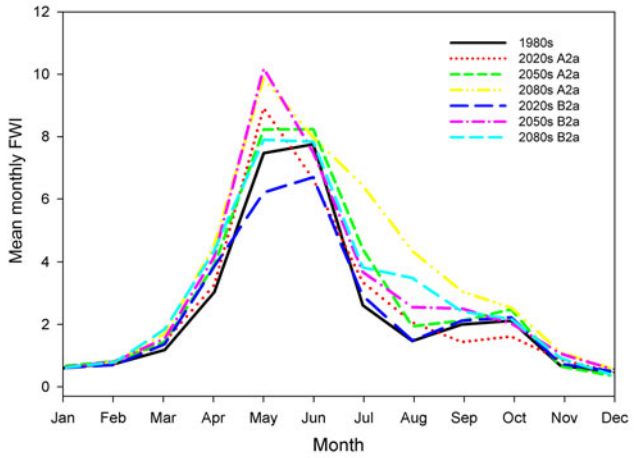

Fig. 8 Mean monthly FWI values for the baseline and three future periods under the two climate change scenarios.

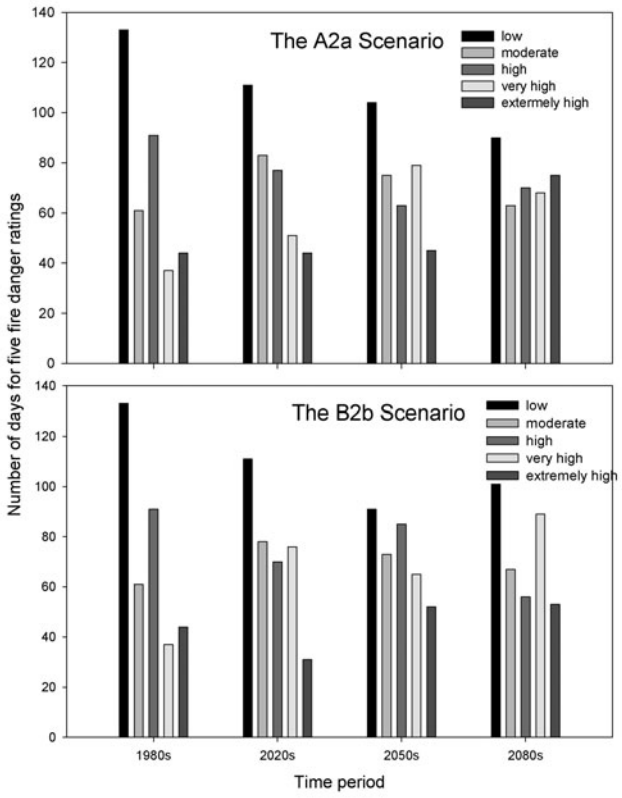

Fig. 9 Number of days with different fire danger ranking for the baseline and three future periods under the two climate change scenarios.

Table 3. Summary of the proportions of fire activities corresponding to the fire danger classes during 1966–2008.

Fire danger class	FWI interval	Proportion of fire activities (%)		
		Occurrence	A B	FAB
Low	[0, 2)	4.30	0.66	0.34
Moderate	[2, 5)	11.30	6.86	1.91
High	[5, 9)	19.91	11.51	11.15
Very high	[9, 16)	32.95	38.27	46.90
Extremely high	[16, ∞)	31.54	42.71	39.71

AB: Area burned; FAB: Forested area burned.

In the study region, both annual mean FWI and annual maximum FWI are predicted to increase by 22%–52% across much of the study region in 2080s under either of the two climate change scenarios. The monthly mean FWI suggests that the study region is going to experience the highest fire danger from March to November in the future periods rather than in the baseline period when the fire danger was highest in spring and autumn. The results also indicate that the monthly mean FWI value could increase by as much as 148% by the end of the 21st century, and the increase would happen in spring and summer. Forest fires that occur on days with high fire danger tend to be large and severe fires. The study indicates that in the future the number of days with extremely high fire danger is going to increase (53–75 days of extreme high danger by 2080s, compared to a present 44 days of the same danger rating). As a result, the proportion of large fires among all fire sizes in the future is very likely to increase.

Under either of climate change scenarios, the FWI in China's boreal forest is going to increase in the three future periods, which indicates that the forest fire danger is going to increase. Such information is an alert to the forest management agencies in the study region. The information on other factors influencing fire ignition and fire behavior such as terrain, vegetation, fuel type and load, topography, transportation network, fire suppression capability, and so forth, should also be helpful to forest management to set up their protection plan. At present the density of meteorological stations is relatively low, the spatial distribution of the stations is uneven and some of the stations are not in the forested area. These factors affect the accuracy of the FWI derivation. Nevertheless, the study results provide important information on the relationship between future fire activities and the impact of climate change on forest fires in China's boreal forest. Our results could also be a helpful reference for similar studies in other boreal forests around the world.

References

Akhtar M, Ahmad N, Booij MJ. 2008. The impact of climate change on the water resources of Hindukush–Karakorum–Himalaya region under different glacier coverage scenarios. *Journal of Hydrology*, **335**:

148–163.

Andrews P, Finney M, Fischetti M. 2007. Predicting wildfires. *Scientific American*, **297**: 47–55.

Chien YJ, Lee DY, Guo HY, Houng KH. 1997. Geostatistical analysis of soil properties of Mid-west Taiwan soils. *Soil Science*, **162**(4): 291–298.

Conard SG, Ivanova GA. 1997. Wildfire in Russian boreal forests-potential impacts of fire regime characteristics on emissions and global carbon balance estimates. *Environmental Pollution*, **98**: 305–313.

Di Xueying. 1993. Forest fire forecast. Harbin: Northeast Forestry University, 161–175. (in Chinese)

Flannigan MD, Harrington JB. 1988. A study of the relation of meteorological variables to monthly provincial area burned by wildfire in Canada (1953-80). *Journal of Applied Meteorology*, **27**(4): 441–452.

Flannigan MD, Amiro BD, Stocks BJ, Wotton BM. 2005. Forest fires and climate change in the 21st century. *Mitigation and Adaptation Strategies for Global Change*, **11**: 847–859.

Flannigan MD, logan KA, Amiro BD, Skinner WR, Stocks BJ. 2005. Future area burned in Canada. *Climatic Change*, 72: 1–16.

Flannigan MD, Stocks BJ, Wotton BM. 2000. Climate change and forest fires. *The Science of the Total Environment*, **262**: 221–229.

Gordon C, Cooper C, Senior CA, Banks H, Gregory JM, Johns TC, Mitchell JFB, Wood RA. 2000. The simulation of SST, sea ice extents and ocean heat transports in a version of the Hadley Center coupled model without flux adjustments. *Climatic Dynamics*, **16**: 147–168.

Hennessy K, Lucas C, Nicholls N, Bathols J, Suppiah R, Ricketts J. 2006. Climate change impacts on fire-weather in south-east Australia. Australia: CSIRO.

Heilongjiang Yearbook Editorial Board. 2008. Heilongjiang yearbook 2008. Harbin: Heilongjiang Yearbook Press Publishing, 488–489. (in Chinese)

Jiang H, Apps MJ, Peng CH, Zhang YL, Liu JX. 2002. Modelling the influence of harvesting on Chinese boreal forest carbon dynamics. *Forest Ecology and Management*, **169**: 65–82.

Johnson EA, 1992. Fire and vegetation dynamics: studies from the North American boreal forest. Cambridge: Cambridge University Press, p3.

Lavorel S, Flannigan MD, Lambin EF, Scholes MC. 2007. Vulnerability of land systems to fire: interactions among humans, climate, the atmosphere, and ecosystems. *Mitigation and Adaptation Strategies for Global Change*, **12**: 33–53.

Leckebusch GC, Ulbrich U. 2004. On the relationship between cyclones and extreme windstorm events over Europe under climate change. *Global and Planetary Change*, **44**: 181–193.

Lv Aifeng, Tian Hanqin. 2007. Interaction among climatic change, fire disturbance and ecosystem productivity. *Journal of Plant Ecology*, **31**(2): 242–251. (in Chinese)

Mollicone D, Eva HD, Achard F. 2006. Ecology: human role in Russian wild fires. *Nature*, **440**: 436–437.

National Bureau of Statistics, Ministry of Civil Affairs. 1995. Report of the damage caused by disaster in China. Beijing: China Statistics Press Publishing, p161–162. (in Chinese)

Pausas JG. 2004. Changes in fire and climate in the eastern Iberian peninsula (Mediterranean Basin). *Climatic Change*, **63**: 337–350.

Pinol J, Terradas J, Lloret F. 1998. Climate warming, wildfire hazard, and wildfire occurrence in coastal eastern Spain. *Climatic change*, **38**: 345–357.

Pope VD, Gallani ML, Rowntree PR, Stratton RA. 2000. The impact of new physical parameterizations in the Hadley Center coupled model without flux adjustments. *Climate Dynamics*, **17**: 61–81.

Richardson CW, Wright DA. 1984. WGEN: a model for generating daily weather variables. U. S. Department of Agriculture, Agricultural Research Service ARS-8, p83.

Running SW. 2006. Is global warming causing more larger wildfires? *Science*, **313**: 927–928.

Semenov MA, Brooks RJ, Barrow EM, Richardson CW. 1998. Comparison of the WGEN and LAR-WG stochastic weather generators for diverse climates. *Climate Research*, **10**: 95–107.

Soja AJ, Tchebakova NM, French NHF, Flannigan MD, Shugart HH, Stocks BJ, Sukhinin AI, Parfenova EI, Stuart CF, Stackhouse PW. 2007. Climate-induced boreal forest change: Predictions versus current observations. *Global and Planetary Change*, **56**: 274–296.

Stocks BJ, Fosberg MA, Lynham TJ, Mearns L, Wotton BM, Yang Q, Jin JZ, Lawrence K, Hartley GR, Mason JA, Mckenney DW. 1998. Climate Change and forest fire potential in Russian and Canadian boreal forests. *Climatic Change*, **38**: 1–13.

Swetnam, TW. 1993. Fire history and climate change in giant sequoia groves. *Science*, **262**: 885–889.

Tian Xiaorui, McRae D, Zhan Youhui. 2006. Assessment of forest fire danger rating systems. *World Forestry Research*, **19**(2): 39–46. (in Chinese)

Tymstra C, Flannigan MD, Armitage OB, Logan K. 2007. Impact of climate change on area burned in Alberta's boreal forest. *International Journal of Wildland Fire*, **16**: 153–160.

Van Wagner CE.1987.Development and structure of the Canadian forest fire weather index system. Ottawa: Canadian Forestry Service, p1–7.

Westerling AL, Hidalgo HG, Cayan DR, Swetnam TW. 2006. Warming and Earlier Spring Increase Western U. S. Forest Wildfire Activity. *Science*, **313**: 940–943.

Wheaton E. 2001. *Changing fire risk in a changing climate: a literature review and assessment*. Saskatchewan: SRC Publishing.

Willis C, Van Wilgen B, Tolhurst K, Everson C, D'Abreton P, Pero L, Fleming G. 2001. The development of a National Fire Danger Rating System for South Africa. Prepared for Department of Water Affairs and Forestry Pretoria Technical Report. CSIR Water by Environment of Forestry Technology.

Yost RS, Uehara G, Fox RL. 1982. Geostatistics analysis of soil chemical properties of large land area. II. Kriging. Soil *Science Society of America Journal*, **46**: 1033–1037.

Zhao Fangfang, Xu Zongxue. 2007. Comparative analysis on downscaled climate scenarios for headwater catchment of yellow river using SDS and delta methods. *Acta Meteorologica Sinica*, **65**(4): 653–661. (in Chinese)